Universality of the Kolmogorov constant in numerical simulations of turbulence

P. K. Yeung
School of Aerospace Engineering, Georgia Institute of Technology, Atlanta, Georgia 30332

Ye Zhou
Institute for Computer Applications in Science and Engineering, NASA Langley Research Center, Hampton, Virginia 23681
and IBM Research Division, T. J. Watson Research Center, P.O. Box 218, Yorktown Heights, New York 10598

(Received 6 January 1997)

Motivated by a recent survey of experimental data [K. R. Sreenivasan, Phys. Fluids **7**, 2778 (1995)], we examine data on the Kolmogorov spectrum constant in numerical simulations of isotropic turbulence, using results both from previous studies and from new direct numerical simulations over a range of Reynolds numbers (up to 240 on the Taylor scale) at grid resolutions up to 512^3. It is noted that in addition to $k^{-5/3}$ scaling, identification of a true inertial range requires spectral isotropy in the same wave-number range. The new simulations indicate approximate inertial range behavior at lower wave numbers than previously thought, with proportionality constants C_1 and C in the one- and three-dimensional energy spectra, respectively, about 0.60 and 1.62. The latter suggests $C_1 \approx 0.53$, in excellent agreement with experiments. However, the one- and three-dimensional estimates are not fully consistent, because of departures (due to numerical and statistical limitations) from isotropy of the computed spectra at low wave numbers. The inertial scaling of structure functions in physical space is briefly addressed. [S1063-651X(97)12708-8]

PACS number(s): 47.27.Ak, 47.27.Gs, 47.27.Jv

I. INTRODUCTION

Inertial-range behavior as postulated by Kolmogorov's (K41) similarity hypotheses [1] is widely regarded as a fundamental characteristic of turbulence at high Reynolds number. In particular, in the inertial range of intermediate scales the K41 result for the one-dimensional longitudinal energy spectrum is given by

$$E_{11}(k_1) = C_1 \langle \epsilon \rangle^{2/3} k_1^{-5/3}, \tag{1}$$

where k_1 is the longitudinal wave number, C_1 is known as the Kolmogorov constant, and $\langle \epsilon \rangle$ is the mean dissipation rate. Although K41 theory is subject to intermittency corrections associated with dissipation rate fluctuations, such effects are primarily manifested in higher-order statistics. Indeed, intermittency effects on the second-order energy spectrum exponent are believed to be small and hardly measurable (Kolmogorov [2], Frisch [3]), while at the same time may contribute to a persistence Reynolds number dependence for higher-order structure functions (L'vov and Procaccia [4]).

The classical view of the ''five-thirds'' scaling law above, with substantial experimental support (e.g., Monin and Yaglom [5], Sec. 23.3), is that C_1 has a universal value at asymptotically high Reynolds number. Recently, however, there is renewed debate on the universality of C_1, in part because of new measurements at high Reynolds number (Praskovsky and Oncley [6]) and a subsequent new similarity theory (Barenblatt and Goldenfeld [7]) that suggested a persistent Reynolds number dependence even at high Reynolds numbers. On the other hand, the conclusion from a new and very extensive survey of experimental data by Sreenivasan [8] is that, taken collectively, measurements do not support such a dependence for the Kolmogorov constant. Sreenivasan found that the value of C_1 averaged over the many different experiments cited is about 0.53 ± 0.055, although some corrections for the estimation of dissipation using local isotropy assumptions in experiments may be warranted. It is still possible (Barenblatt and Goldenfeld [7], Sreenivasan [8]), though, that controlled experiments for a single geometry over a wide range of Reynolds numbers may reveal significant trends otherwise masked by experimental scatter; new measurements of this nature (suggesting strong Reynolds number dependence) have been reported by Mydlarski and Warhaft [9].

This paper is motivated by the survey of experimental data noted above, and will focus on similar issues arising in numerical simulations of isotropic turbulence. We first review the basis for estimating the Kolmogorov constant from previous studies, and then present new results from direct numerical simulations (DNS's) over a range of Reynolds numbers. Because of Reynolds number considerations, an accurate evaluation of the Kolmogorov constant by DNS is admittedly very difficult. As such, we limit ourselves to the task of providing new insights on the interpretation of K41 similarity in the DNS literature. For similar reasons, we shall not consider the use of DNS to study issues pertaining to the refined similarity hypotheses of Kolmogorov (K62) [2] (see, e.g., Chen *et al.* [10], Wang *et al.* [11], and others).

In numerical simulations, K41 similarity is frequently discussed in terms of the three-dimensional energy spectrum function $E(k)$ (where k is the wave-number magnitude). If the turbulence at scale size $1/k$ is isotropic then a kinematic constraint relating one- and three-dimensional spectra is

$$E(k) = \frac{1}{2} k^3 \frac{d}{dk} \left(\frac{1}{k} \frac{dE_{11}(k)}{dk} \right). \tag{2}$$

TABLE I. Kolmogorov constant computed from DNS and LES. (We included most of the recent numerical data on the Kolmogorov constant.)

Authors	Method	Grid	R_λ	C (1D)[a]	C (3D)
Lesieur and Rogallo [12]	Forced LES[b]	128^3			1.5–1.8
Chasnov [13]	Forced LES[c]	128^3			2.1
Zhou [14]	LES[d]	256^3			1.5
She and Jackson [15]	LES[e]	128^3			1.88
Borue and Orszag [16]	LES[f]	256^3		1.2–1.7	1.2–1.4
Kerr [17]	Forced DNS	128^3	82		2
Vincent and Meneguzzi [18]	Forced DNS	240^3	150		2
Sanda [19]	Forced DNS	256^3	120		2
Jiménez *et al.* [20]	Forced DNS	512^3	170−	0.91–1.22	2
Wang *et al.* [11]	Forced DNS[g]	512^3	190	1.68	1.5–2
Hosokawa *et al.* [21]	DNS	512^3	160	2.1	
Present study	Forced DNS	512^3	240	1.83	1.62

[a]C (1D) is obtained as $(55/18)C_1$, assuming isotropy in the inertial range. (Hosokawa *et al.* used $0.76C_2$, from the structure function.)
[b]Spectral LES with a spectral eddy viscosity.
[c]Spectral LES with an eddy viscosity and a stochastic force.
[d]Zhou used simulation databases from a constrained energy simulation where a ''five-thirds'' spectrum is maintained. Furthermore, the self-similarity condition is used to compute an ideal Kolmogorov energy transfer function. The Kolmogorov constant is determined from the flux.
[e]She and Jackson used the constrained Euler system simulation. The Kolmogorov constant is determined from the flux.
[f]Borue and Orszag reported their decaying DNS at 256^3 resolution along with a hyperviscosity. Both C (1D) and C (3D) are estimated by the authors of the present paper from Fig. 4 of [16]. The contributions from the ''bumps'' are ignored.
[g]Wang *et al.* argued that the Kolmogorov constant is more accurate when estimated from C (1D) followed by using the isotropy relation.

Substitution of Eq. (1) into Eq. (2) implies that in the inertial range

$$E(k)=C\langle\epsilon\rangle^{2/3}k^{-5/3}, \tag{3}$$

where $C=55/18\,C_1$. In principle, therefore, one may obtain either C or C_1 (from three- and one-dimensional spectra, respectively) and infer the other using isotropy relations. Values of the Kolmogorov constant C (estimated using either of these approaches) cited in a number of recent high resolution numerical studies by other authors [11–21] are collected in Table I. Some relevant results from large-eddy simulations (LES's) are included also. (Note that we have quoted values of C from the highest-resolution data in each of these references, since from the viewpoint of present paper we should not infer the Kolmogorov constant from low-resolution simulations, especially in the older data.)

It may be noticed that most of the values displayed in Table I are higher than the value 1.619, which is 55/18 of the experimental average of 0.53 for C_1. Note that, however, Zhou [14] found that the Kolmogorov constant $C=1.5$ from calculations of the spectra energy flux based on the self-similarity condition of the triadic energy transfer function, in the form $T(k,p,q)=a^3T(ak,ap,aq)$ (where a is a scaling constant). A commonly used procedure (e.g., Kerr [17], Jiménez *et al.* [20]) for estimating the value of C is to plot the ''compensated'' three-dimensional energy spectrum

$$\psi(k)\equiv E(k)\langle\epsilon\rangle^{-2/3}k^{5/3} \tag{4}$$

as a function of wave number normalized by the Kolmogorov scale (η), and to interpret C as the height of a ''plateau.'' However, it should be noted that whereas a flat region in the compensated spectrum implies $k^{-5/3}$ behavior, the observation of a $k^{-5/3}$ scaling range is not by itself a sufficient condition for an inertial range. It is important that isotropy also be attained in the wave-number range which displays $k^{-5/3}$ behavior. (If the isotropy requirement were relaxed then, in principle, one would have a different value of the ''Kolmogorov constant'' in each direction, and the concept of universality would be lost.) Indeed, as will be seen in the rest of this paper, our new results demonstrate that deviations from isotropy can contribute to values of C that appear to be too high.

The major limitation in using DNS to examine inertial-range dynamics is, of course, the difficulty in attaining high Reynolds numbers. However, recent advances in massively parallel computing have shown significant promise. Our simulations were performed using a parallel implementation [22] of the well-known Fourier pseudospectral algorithm of Rogallo [23] on the IBM SP at the Cornell Theory Center. The highest grid resolution used is 512^3, with a Taylor-scale Reynolds number (R_λ) about 240 averaged over about four eddy-turnover times. Whereas this Reynolds number is not high compared to some recent laboratory experiments (R_λ 473 in Mydlarski and Warhaft [9]), it is about the same as (or slightly higher than) the highest values reported in the DNS literature (for example, R_λ 218 in Cao *et al.* [24]). Numerical results on spectra as well as structure functions (to which Kolmogorov [1] originally referred) are given in the next section. In order to characterize issues of Reynolds number dependence and attempt to quantify a minimum Reynolds number threshold above which inertial-range behavior could be expected, we present data at five different grid resolutions.

TABLE II. Major simulation parameters in the new results. Note that T is the total averaging time period, and T_E is the eddy-turnover time (the ratio of the longitudinal integral length scale, L_1, to the rms velocity fluctuation, u').

Grid	R_λ	T/T_E	$\langle\epsilon\rangle L_1/u'^3$
64^3	38	146	0.693
128^3	90	139	0.499
256^3	140	9.8	0.475
384^3	180	3.2	0.419
512^3	240	3.9	0.416

To maintain a stationary state so that results may be averaged over time at the highest Reynolds number possible using a given number of grid points, it is usual to apply numerical forcing at the large scales. In the literature this has been done in several different ways, such as adding a stochastic forcing term (Eswaran and Pope [25]), holding the energy in the lowest-wave-number shells fixed while allowing phase information to evolve (Chen *et al.* [10], Sullivan *et al.* [26]), or by introducing a negative viscosity in these shells (Jiménez *et al.* [20]). Alternatively, LES [12–15], with and without forcing, as well as simulations with a hyperviscosity [16] can also be used to achieve higher Reynolds numbers. However, it is generally believed that (e.g., see [20]), the precise manner of forcing—provided it is applied to the largest scales in the flow—has no systematic effects on the inertial-range energy spectrum, nor on the statistical character of the small scales. Whereas in this work we have used the scheme of Eswaran and Pope [25], we have checked that similar calculations in which the energy in the first couple of wave-number shells is fixed do not warrant different conclusions.

II. RESULTS

We present spectra and structure functions from simulations of forced stationary isotropic turbulence averaged over relatively long time periods. Major simulation parameters are summarized in Table II. For the less expensive 64^3 and 128^3 runs the averaging time (T) shown is the aggregate of multiple simulations of shorter duration. In all cases the small scales are considered to be well resolved, as measured by $k_{\max}\eta \approx 1.5$, where $k_{\max}$ is the highest wave number represented by the grid points. The nondimensional quantity $\langle\epsilon\rangle L_1/u'^3$ (where L_1 is the longitudinal integral length scale derived from the longitudinal velocity correlation, and u' is the rms velocity) in the last column of this table is of interest in the scaling of $\langle\epsilon\rangle$ with u'^3/L_1 using energy cascade arguments; it appears to approach a constant at high Reynolds numbers. This trend is similar to that found in the simulations of Jiménez *et al.* [20], Wang *et al.* [11], and Cao *et al.* [24], and to that in experiments (Sreenivasan [27], Fig. 1). The differences among different ''asymptotic'' numerical values are due in part to differences in the definition of integral scales and in flow conditions in experiments and numerical simulations.

Figure 1 shows the three-dimensional compensated spectrum $\psi(k)$ in Kolmogorov scaling. (Note that in these and all other figures lines $A-E$ refer to data at five different grid resolutions from 64^3 to 512^3 respectively, as listed in Table II.) Except for small spectral turnups at the high-wave-number end resulting from residual aliasing errors, small-scale universality is unambiguously achieved, even at the lowest Reynolds number (R_λ 38 in 64^3 simulations). Two relatively flat (i.e., $k^{-5/3}$) regimes of limited extent can be seen: namely at $k\eta \approx 0.1-0.2$ in the form of a bumpy ''plateau'' which is seen at all grid resolutions, and in the low-wave-number range $k\eta \approx 0.02-0.05$ which is captured only at higher (256^3 and beyond) resolutions. If the former were taken to represent the inertial range then one would obtain a Kolmogorov constant C greater than 2.0, as reported by a number of other authors (see Table I). On the other hand, it is clear that the level of $\psi(k)$ in the range $k\eta \approx 0.02-0.05$ agrees well with experimental data, if one uses the isotropy relation $C = 55/18\, C_1$, which would imply $C_1 = 18/55\ C \approx 0.53$. It is our objective in the analyses below to establish that this lower-wave-number region, rather than the plateau, represents (the beginnings of) a proper inertial range.

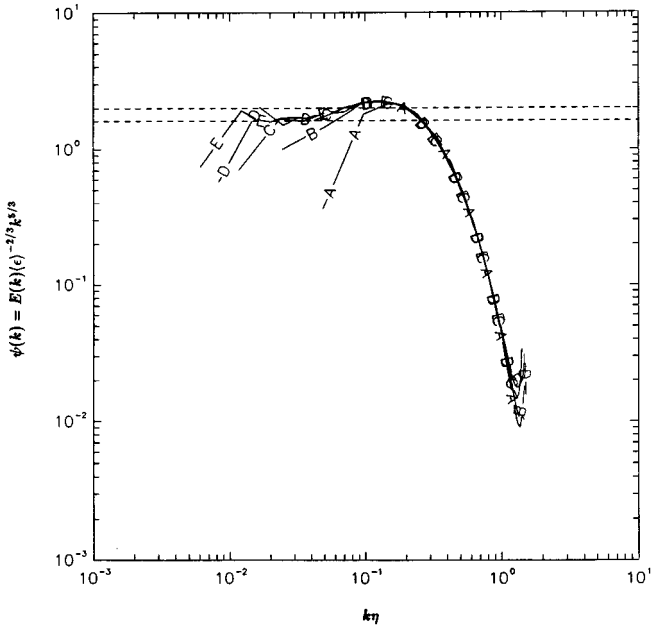

FIG. 1. Compensated three-dimensional energy spectrum $\psi(k)$ vs Kolmogorov-scaled wave number $k\eta$, at five different Reynolds numbers and grid resolutions (see Table II). Dashed horizontal lines at levels $1.619 = (55/18)0.53$ and 2.0 are drawn for reference.

In order that inertial range dynamics can be independent of both the large-scale energetics and viscous dissipation, a wide scale separation must exist between the peaks of the energy and dissipation spectra in wave-number space. The peak of $E(k)$ occurs in the lowest two wave-number shells ($k\eta \approx 0.01$ for the 512^3 data), whereas from a plot of the dissipation spectrum we find that the peak of $D(k) \equiv 2\nu k^2 E(k)$ occurs at $k\eta \approx 0.17$. This location of the dissipation spectral peak is virtually the same as found by She *et al.* [28] and Wang *et al.* [11]. Since this almost coincides with the ''plateau'' in Fig. 1 it is clear that the plateau should not be taken as an indication of inertial-range behavior. In fact, this plateau may be identified with the so-called ''bottleneck'' phenomenon that has been discussed in experimental (Saddoughi and Veeravalli [29]), theoretical (Falkov-

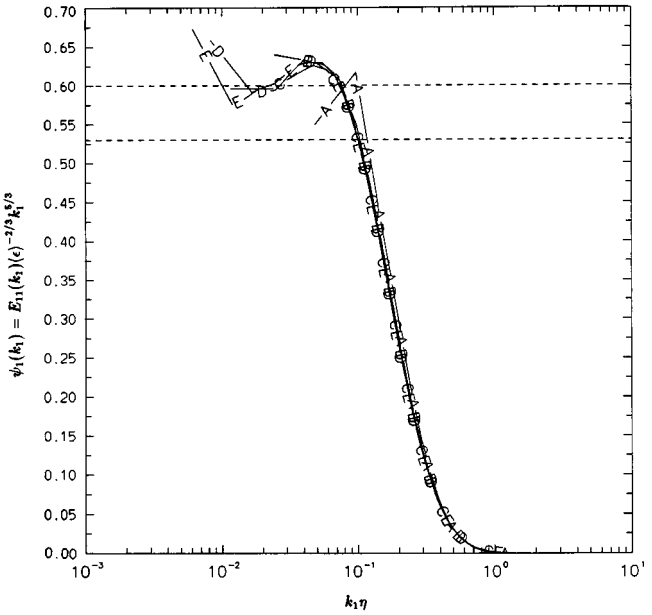

FIG. 2. Compensated one-dimensional energy spectrum vs Kolmogorov-scaled wave number $k_1\eta$, at five different Reynolds numbers and grid resolutions (see Table II). The reference lines are drawn at levels 0.53 and 0.60.

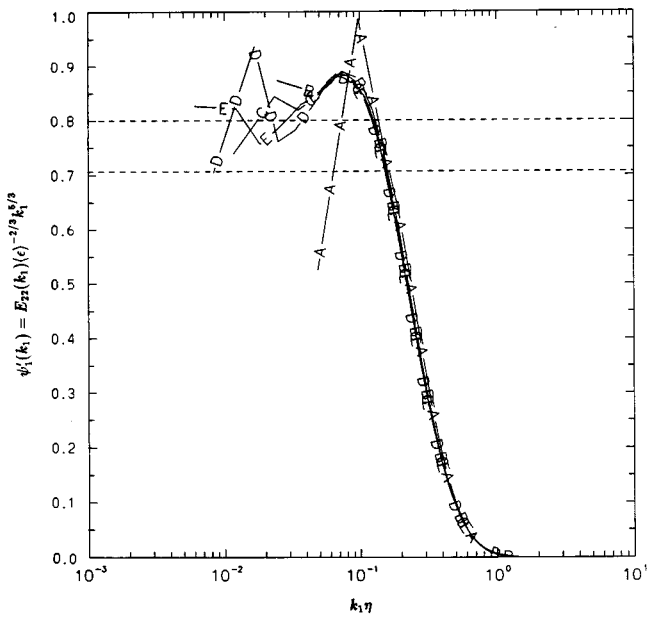

FIG. 3. Same as Fig. 2, but for the transverse spectrum. The reference lines are drawn at levels $0.707=(4/3)0.53$ and 0.8.

ich [30]), and numerical (Borue and Orszag [31]) work. According to this theory, viscous effects on spectral transfer causes an increase (relative to $k^{-5/3}$) in the energy spectrum at intermediate wave numbers. Nonlocal interactions among Fourier modes well separated in scale (Brasseur and Wei [32]) are also believed to play an important role (Herring *et al.* [33]). We also note that Brasseur and Wei argued that there should be about a decade in scale separation between the wave number where the inertial range ''ends'' and the dissipation peak, which is more than that (about 3 to 4) found in DNS (Wang *et al.* [11] and this paper). A full understanding of this latter issue awaits future high-resolution simulations and experimental data.

A more direct comparison with experiment may be made by considering the compensated longitudinal energy spectrum, i.e., $\psi_1(k_1)=E_{11}(k_1)\langle\epsilon\rangle^{-2/3}k_1^{5/3}$, which is shown in Fig. 2. Because this spectrum drops off very rapidly at high wave numbers, we have used log-linear scales to highlight the function values at any wave-number ranges where ψ_1 is approximately constant. Two such ranges can be seen, corresponding to those for ψ but in each case occurring at lower wave numbers. The observation that the peak of $\psi_1(k_1)$ occurs at $k_1\eta=0.05$ is similar to high Reynolds number measurements in both boundary layers (Saddoughi and Veeravalli [29]) and grid turbulence (Mydlarski and Warhaft [9]). It is also apparent that the value of C_1 inferred from this figure is about 0.60, which is somewhat higher than, but still relatively close to the experimental average [5] of 0.53.

From Figs. 1 and 2 we may conclude that the best values obtained for C_1 from the three- and one-dimensional spectra are about 0.53 and 0.60, respectively. These values (especially the former) are closer to experiment than those cited previously in the literature. Yet there is evidently some inconsistency between these two estimates for C_1. These differences are due to deviations from isotropy in wave-number space, as further studied below.

In addition to $E_{11}(k_1)$ we have also computed the transverse energy spectrum, for which the classical inertial-range result is

$$E_{22}(k_1)=C_1'\langle\epsilon\rangle^{2/3}k_1^{-5/3}, \tag{5}$$

where isotropy requires $C_1'=\frac{4}{3}C_1$. The compensated transverse spectrum (Fig. 3) exhibits a similar but stronger bump at $k_1\eta\approx0.07$. We also find that the ratio $E_{22}(k_1)/E_{11}(k_1)$ is close to 4/3 in the range $k_1\eta\approx0.02-0.04$, but increases steadily with wave number beyond this range.

If a five-thirds scaling holds for both one- and three-dimensional spectra over the *same* wave-number range then the functions $E(k)$ and $E_{11}(k)$ should be proportional within this range. Figure 4 shows the spectral ratio $E(k)/E_{11}(k)$, compared with the classical inertial range value of 55/18. It may be seen that, at the wave-number range ($k\eta\approx0.1-0.2$) corresponding to the plateau in Fig. 1, this ratio is considerably higher than 55/18 and in fact increases roughly in proportion to $k\eta$. This observation provides further evidence that the plateau in ψ does not represent an inertial range. The transition from behavior without a level region to one at a value close to 55/18 (at R_λ 240 at 512^3 resolution) occurs between R_λ 90 (on an 128^3 grid) and R_λ 140 (for 256^3). The ratio C/C_1 inferred in this manner is seen to be somewhat less than 55/18.

It should be noted that isotropy of the spectral tensor is a key requirement for the relation $C=55/18C_1$. Although the simulations are of (nominally) isotropic turbulence, departures of the computed spectra from isotropy are, in fact, not totally unexpected. It is well known that sampling limitations arise in the lowest few wave-number shells because relatively few samples of the large scales are present in a solution domain of finite size. Furthermore, since the solution

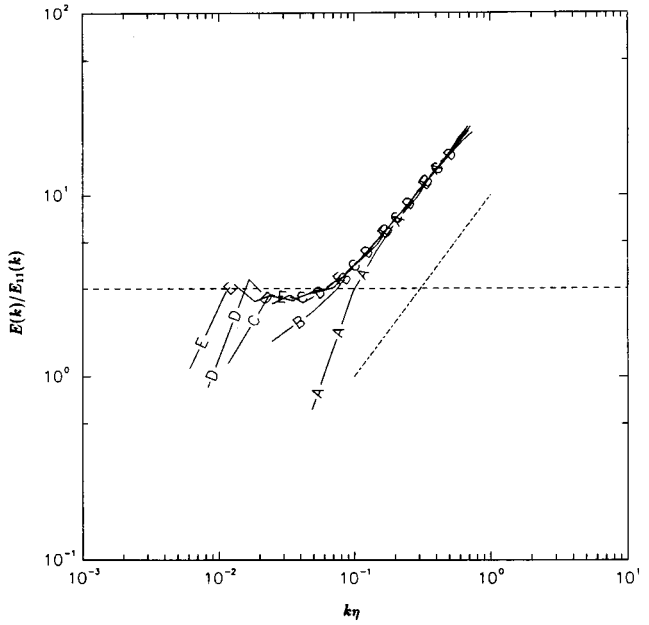

FIG. 4. The ratio $E(k)/E_{11}(k)$ vs Kolmogorov-scaled wave number. The horizontal line is at 55/18, whereas the sloping line has slope unity. Because this ratio attains very large values at high wave numbers, only the lower half of the wave-number range in each simulation is shown.

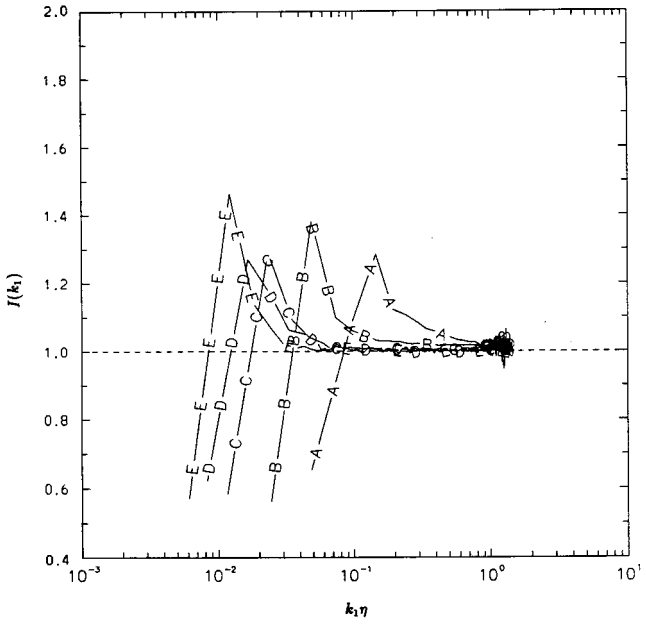

FIG. 5. The isotropy coefficient $I(k_1)$ [see Eq. (6)] vs Kolmogorov-scaled one-dimensional wave number. (A value of unity signifies spectral isotropy.)

domain in physical space is a cube (rather than a sphere), the averaged statistics are at best invariant among the three Cartesian coordinate axes, but do not satisfy the stricter requirement of no preferential orientation in three-dimensional space. As an example we may note that whereas the periodicity length of the flow along the coordinate axes is equal to the length of each side of the solution domain, it is longer if measured along directions inclined to the axes. This effect is felt primarily in spatial correlations over large separations in space, which correspond to low wave numbers in Fourier space.

Following Jiménez *et al.* [20], as a test of spectral isotropy, in Fig. 5 we plot an ''isotropy coefficient''

$$I(k_1)\equiv\frac{E_{11}(k_1)-k_1E_{11}(k_1)/dk_1}{2E_{22}(k_1)}, \tag{6}$$

which should be equal to unity if the spectra were strictly isotropic. The results are similar to those of Jiménez *et al.* (who used a different forcing scheme), although we have apparently achieved improved isotropy at the small scales. At low wave numbers we observe significant deviations from isotropy in all simulations. In particular, at wave numbers that best resemble an inertial range ($k_1\eta\approx 0.2-0.4$) in the high-resolution simulations, we find departures from isotropy on the order 10%, which would explain at least in part the observed departure from the result $C=55/18\,C_1$. For a given $k_1\eta$ it is also seen that agreement with isotropy improves with increasing resolution, which causes the respective scale size to become smaller compared to the solution domain. The value of $I(k_1)$ at the lowest k_1 in each simulation is systematically less than 1.0: this can be traced to the constraints placed on two-point correlations by the use of periodic boundary conditions. Note that similar conclusions are obtained from the use of another isotropy coefficient (Borue and Orszag [16]) which is based on Eq. (2) relating one- and three-dimensional spectra. A more rigorous analysis of spectral isotropy could also be made based on principal anisotropy invariants of the spectrum tensor (Yeung *et al.* [34]). Whereas we have not collected sufficient data to compute this information from the high-resolution runs, results from 64^3 runs do show similar departures from anisotropy in the lowest few wave-number shells.

Despite the observed departures from isotropy, it can be argued that the higher-resolution (256^3 and beyond) spectra shown in this paper do represent approximate inertial-range behavior. For a corresponding description in physical space we include results for the structure functions as a function of spatial separation r. It is well known that the inertial-range forms for the second- and third-order longitudinal structure functions are

$$D_{LL}(r)=C_2\langle\epsilon\rangle^{2/3}r^{2/3}, \tag{7}$$

where $C_2\approx 4.02C_1$ from isotropy and

$$D_{LLL}(r)=-\frac{4}{5}\langle\epsilon\rangle r. \tag{8}$$

In Figs. 6 and 7 these structure functions are shown in Kolmogorov scaling in order to compare with the theoretical proportionality constants $C_2\approx 4.02\,C_1$ and $-4/5$. It is clear that the highest Reynolds number data shown agree well with classical inertial range results. Numerical values of $-D_{LLL}(r)/\langle\epsilon\rangle r$ at intermediate resolutions also fit in well

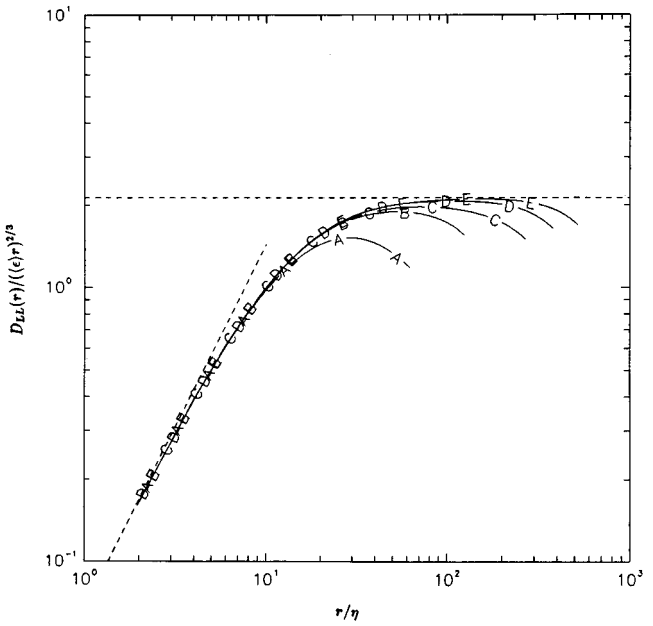

FIG. 6. Kolmogorov scaling of the second-order longitudinal structure function. The horizontal line is at $2.13=(4.02)(0.53)$; the sloping dashed line indicates universal behavior of the small scales, as $(1/15)(r/\eta)^{4/3}$.

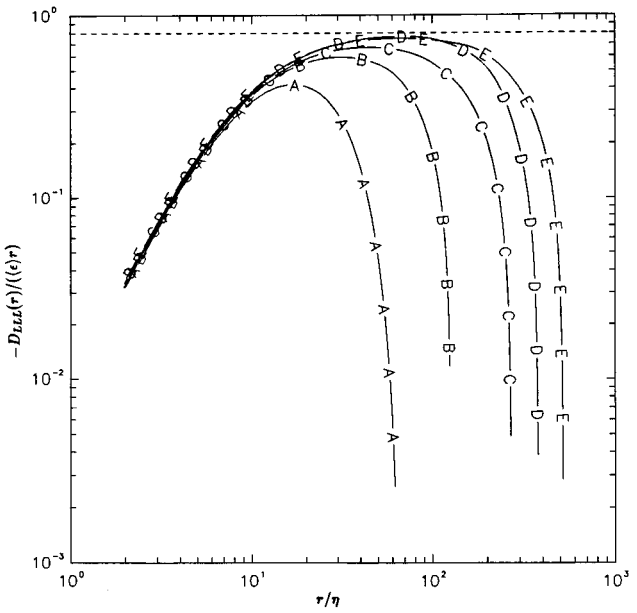

FIG. 7. Kolmogorov scaling of the third-order longitudinal structure function. The horizontal line is at 0.8.

within the Reynolds number trend suggested by new measurements in grid turbulence over a range of Reynolds numbers (Sreenivasan and Dhruva [35]).

It is perhaps worth noting that the highest-resolution (512^3) simulation reported is at a higher Reynolds number and are averaged over a greater number of large-eddy turnover times than several other studies reporting 512^3 results (e.g., Jiménez *et al.* [20], Chen *et al.* [10], and Wang *et al.* [11]) for stationary isotropic turbulence. The spectra and structure functions obtained from these and the present simulations demonstrate that, with the latest advances in massively parallel computing, issues concerning inertial-range similarity in DNS can now be addressed in a more reliable manner than possible before.

III. CONCLUSIONS AND DISCUSSION

We have presented new results on the Kolmogorov scaling of energy spectra and structure functions in the inertial range, from direct numerical simulations of stationary isotropic turbulence ranging from R_λ 38 (on a 64^3 grid) to R_λ 240 (on 512^3). It is pointed out that a plateau in the compensated three-dimensional energy spectrum at $k\eta \approx 0.1-0.2$ commonly used to infer the Kolmogorov constant from the compensated three-dimensional energy spectrum in fact does not represent proper inertial range behavior. Instead, a proper (if still approximate) inertial range emerges at $k\eta \approx 0.02-0.05$ when R_λ increases beyond 140. We find that the proportionality constants C and C_1 in the three- and one-dimensional compensated energy spectra are about 1.62 and 0.60, respectively. These values are closer to experimental data than reported in most previous numerical simulations. In particular, if isotropy relations are used then we may infer from the three-dimensional spectra that $C_1 = 18/55$ $C \approx 0.53$, in excellent agreement with experimental data (Sreenivasan [8]). However, the ratio C/C_1 in our results differs from the theoretical value of 55/18, because of significant departures from isotropy in the computed spectra at the wave-number range where inertial-range behavior is otherwise reasonably well approximated. Results on second- and third-order structure functions over a range of Reynolds numbers further suggest that the simulation database that we have accumulated should be useful for investigating other aspects of similarity scaling and Reynolds number dependence.

We emphasize that a $k^{-5/3}$ scaling is in itself not a sufficient indicator of inertial-range behavior. To achieve a strictly isotropic inertial range in direct numerical simulations requires that the inertial scales be small compared to the size of the solution domain. Whereas it is difficult to meet this requirement well, it seems clear that high-resolution simulations using the techniques of massively parallel computing are very helpful.

ACKNOWLEDGMENTS

We are grateful to Professor K. R. Sreenivasan for many stimulating discussions and his constant encouragement, as well as comments on an early draft of this paper. In addition, we thank Professor Jim Brasseur, Professor Zellman Warhaft, Dr. Shiyi Chen, and Dr. Jack Herring for their valuable input. This research was supported in part by NSF Grant No. CTS-9307973 to the first author, and by NASA under Contract No. NAS1-19480 while the second author was in residence at ICASE. Figures 6 and 7 evolved from joint work between the first author and Dr. Michael Borgas, within NSF Grant No. INT-9526868. The computations were performed using the supercomputing resources of the Cornell Theory Center, which receives major funding from NSF and New York State.

[1] A. N. Kolmogorov, Dokl. Akad. Nauk SSSR **30,** 301 (1941).
[2] A. N. Kolmogorov, J. Fluid Mech. **13**, 82 (1962).
[3] U. Frisch, *Turbulence: The Legacy of A. N. Kolmogorov* (Cambridge University Press, Cambridge, England, 1995).
[4] V. S. L'vov and I. Procaccia, Phys. Rev. Lett. **74**, 2690 (1995).
[5] A. S. Monin and A. M. Yaglom, *Statistical Fluid Mechanics* (MIT Press, Cambridge, MA, 1975), Vol. II.
[6] A. Praskovsky and S. Oncley, Phys. Fluids **6**, 2886 (1994).
[7] G. I. Barenblatt and N. Goldenfeld, Phys. Fluids **7**, 3078 (1995).
[8] K. R. Sreenivasan, Phys. Fluids **7**, 2778 (1995).
[9] L. Mydlarski and Z. Warhaft, J. Fluid Mech. **320**, 331 (1996).
[10] S. Chen, G. D. Doolen, R. H. Kraichnan, and Z-S. She, Phys. Fluids A **5**, 458 (1993).
[11] L. P. Wang, S. Chen, J. G. Brasseur, and J. C. Wyngaard, J. Fluid Mech. **309**, 113 (1996).
[12] M. Lesieur and M. R. S. Rogallo, Phys. Fluids A **1**, 718 (1989).
[13] J. R. Chasnov, Phys. Fluids A **11**, 945 (1991).
[14] Y. Zhou, Phys. Fluids A **5**, 2524 (1993).
[15] Z.-S. She and E. Jackson, Phys. Rev. Lett. **70**, 1255 (1990).
[16] V. Borue and S. A. Orszag, Phys. Rev. E **51**, R856 (1995).
[17] R. M. Kerr, J. Fluid Mech. **211**, 309 (1990).
[18] A. Vincent and M. Meneguzzi, J. Fluid Mech. **225**, 1 (1991).
[19] T. Sanada, Phys. Fluids A **4**, 1086 (1992).
[20] J. Jiménez, A. A. Wray, P. G. Saffman, and R. S. Rogallo, J. Fluid Mech. **255**, 65 (1993).
[21] I. Hosokawa, S. Oide, and K. Yamamoto, Phys. Rev. Lett. **77**, 4548 (1996).
[22] P. K. Yeung and C. A. Moseley, in *Parallel Computational Fluid Dynamics: Implementations and Results Using Parallel Computers*, edited by A. Ecer, J. Periaux, N. Satofuka, and S. Taylor (Elsevier, Amsterdam, 1995), p. 473.
[23] R. S. Rogallo, NASA, Ames Research Center Technical Memo No. 81315, 1981 (unpublished).
[24] N. Cao, S. Chen, and G. D. Doolen (unpublished).
[25] V. Eswaran and S. B. Pope, Comput. Fluids **16**, 257 (1988).
[26] N. P. Sullivan, S. Mahalingham, and R. M. Kerr, Phys. Fluids **6**, 1612 (1994).
[27] K. R. Sreenivasan, Phys. Fluids **27**, 1048 (1984).
[28] Z.-S. She, S. Chen, G. Doolen, R. H. Kraichnan, and S. A. Orszag, Phys. Rev. Lett. **70**, 3251 (1993).
[29] S. G. Saddoughi and S. V. Veeravalli, J. Fluid Mech. **268**, 333 (1994).
[30] G. Falkovich, Phys. Fluids **6**, 1411 (1994).
[31] V. Borue and S. A. Orszag, J. Fluid Mech. **306**, 293 (1996).
[32] J. G. Brasseur and C-H. Wei, Phys. Fluids **6**, 842 (1994).
[33] J. R. Herring, D. Schertzer, M. Lesieur, G. R. Newman, J. P. Chollet, and M. Larcheveque, J. Fluid Mech. **124**, 411 (1982).
[34] P. K. Yeung, J. G. Brasseur, and Q. Wang, J. Fluid Mech. **283**, 43 (1995).
[35] K. R. Sreenivasan and B. Dhruva (private communication).